COPY RESOLUTION TEST CHART
NATIONAL BUREAU OF STANDARDS — 1963 —

④

AD-A192 154

Deep Dielectric Charging Effects Due to High Energy Electrons in Earth's Outer Magnetosphere

D. N. BAKER, R. D. BELIAN, P. R. HIGBIE, and R. W. KLEBESADEL
Los Alamos National Laboratory
Los Alamos, NM 87545

and

J. B. BLAKE
Space Sciences Laboratory
The Aerospace Corporation
El Segundo, CA 90245

DTIC
ELECTE
S
MAR 0 7 1989
D

5 February 1988

Prepared for

SPACE DIVISION
AIR FORCE SYSTEMS COMMAND
Los Angeles Air Force Base
P.O. Box 92960, Worluway Postal Center
Los Angeles, CA 90009-2960

88 3 5 085

AD A192154

REPORT DOCUMENTATION PAGE

1a REPORT SECURITY CLASSIFICATION	1b. RESTRICTIVE MARKINGS
Unclassified	
2a. SECURITY CLASSIFICATION AUTHORITY	3. DISTRIBUTION / AVAILABILITY OF REPORT
	Approved for public release;
2b. DECLASSIFICATION / DOWNGRADING SCHEDULE	distribution unlimited.

4. PERFORMING ORGANIZATION REPORT NUMBER(S)	5. MONITORING ORGANIZATION REPORT NUMBER(S)
TR-0086A(2940-05)-1	SD-TR-88-08

6a. NAME OF PERFORMING ORGANIZATION	6b. OFFICE SYMBOL (If applicable)	7a. NAME OF MONITORING ORGANIZATION
The Aerospace Corporation Laboratory Operations		Space Division

6c. ADDRESS (City, State, and ZIP Code)	7b ADDRESS (City, State, and ZIP Code)
El Segundo, CA 90245	Los Angeles Air Force Base Los Angeles, CA 90009-2960

8a. NAME OF FUNDING / SPONSORING ORGANIZATION	8b. OFFICE SYMBOL (If applicable)	9. PROCUREMENT INSTRUMENT IDENTIFICATION NUMBER
		F04701-85-C-0086-P00016

8c. ADDRESS (City, State, and ZIP Code)	10 SOURCE OF FUNDING NUMBERS			
	PROGRAM ELEMENT NO.	PROJECT NO.	TASK NO.	WORK UNIT ACCESSION NO.

11 TITLE (Include Security Classification)

Deep Dielectric Charging Effects Due to High Energy Electrons in Earth's Outer Magnetosphere

12 PERSONAL AUTHOR(S)
Baker, D.N., Belian, R.D., Higbie, P.R., Klebesadel, R.W., and Blake, J.B.

13a. TYPE OF REPORT	13b. TIME COVERED FROM _____ TO _____	14. DATE OF REPORT (Year, Month, Day) 1988, February 5	15 PAGE COUNT 28

16. SUPPLEMENTARY NOTATION

17	COSATI CODES		18 SUBJECT TERMS (Continue on reverse if necessary and identify by block number)
FIELD	GROUP	SUB-GROUP	Solar wind
			Terrestrial magnetic
			fields

Solar wind   Dipole fields   Galactic cosmic
Terrestrial magnetic   Van Allen belts   rays
fields   Spectrometer   Solar flares

19 ABSTRACT (Continue on reverse if necessary and identify by block number)

Many spacecraft operational problems in Earth's outer magnetosphere appear to be due to intense, transient radiation phenomena. Three types of naturally occurring, and highly variable, hostile particle radiation environments are encountered at, or near, the geostationary orbit: (1) high-energy protons due to solar flares; (2) energetic ions and electrons produced by magnetospheric substorms; and (3) very high energy electrons of uncertain origin. In this report, particular emphasis is given to highly relativistic electrons, (3 ~ 10 MeV). Electron fluxes and energy spectra are shown which were measured by two high-energy electron sensor systems at 6.6 R_E from 1979 through 1984. Large, persistent increases in this population were found to be relatively infrequent and sporadic in 1979-81 around solar maximum. During the approach to solar minimum (1981 - present), it is observed that the highly relativistic electrons occur with a regular 27-day periodicity and are well associated with the re-established solar wind stream structures. Through a superposed epoch analysis technique, we show that an energetic electron enhancement typically rises on a 2- to

20. DISTRIBUTION / AVAILABILITY OF ABSTRACT	21 ABSTRACT SECURITY CLASSIFICATION
☑ UNCLASSIFIED/UNLIMITED ☐ SAME AS RPT ☐ DTIC USERS	
22a NAME OF RESPONSIBLE INDIVIDUAL	22b TELEPHONE (Include Area Code) 22c OFFICE SYMBOL

DD FORM 1473, 84 MAR   83 APR edition may be used until exhausted
All other editions are obsolete

19. ABSTRACT (Continued)

3-day time scale and decays on a 3- to 4-day time scale at essentially all energies above ~ 3 MeV. The present analysis suggests that these electrons have a very deleterious influence on spacecraft systems due to deep dielectric charging and low-dose susceptibility effects.

CONTENTS

FIGURES

2

I. INTRODUCTION

The magnetosphere is a very tenuous gas of charged particles (a plasma) controlled largely by the terrestrial magnetic field. These terrestrial fields are confined and distorted by the continual flow of hot coronal gases (the solar wind) past the earth. The solar wind confines the earth's magnetosphere to a region extending to ~60,000 km (~ 10 earth radii, R_E) on the dayside and extending hundreds of R_E on the nightside. Thus, most earth-orbiting spacecraft operate for a large part of the time in the earth's magnetosphere.

The relatively strong magnetic field of the terrestrial system is able to confine and trap large fluxes of quite energetic ions and electrons. Very near the earth the magnetic field is well-described by a dipole field, and particles can be durably trapped for very long periods. These are the terrestrial (Van Allen) radiation belts and they constitute a significant radiation hazard to systems in space. Further out in the magnetosphere, the fields are weaker and more variable. There, the radiation shows much greater fluctuations; through this outer region solar cosmic rays, galactic cosmic rays, and particles from other planets (e.g., Jupiter), can enter the magnetosphere and even reach the earth, depending on their energy and direction of approach.

Modern satellite systems, weather and global communication installations, and many defense programs have become dependent on knowledge of the condition of the near-earth space environment. Military spacecraft, commercial satellites, and a wide variety of other scientific and operational space systems require information about solar and ionospheric conditions, magnetospheric disturbance levels, and solar and galactic cosmic ray fluxes. Without such knowledge, these systems cannot operate effectively.

A particularly important aspect of the solar-terrestrial environment is its possibility of producing operational anomalies in spacecraft. The radiation dose effect of flying continually or repeatedly through the trapped radiation belts produces one of the clearest effects on spacecraft operations. Since the inner radiation zones are very stable with time, they may be very

3

well modeled.[1] By a numerical integration of the radiation dose, one may accurately estimate the effects of the radiation belts on a spacecraft having a well-prescribed orbit.

The geostationary orbit (6.6 R_E) is on the outer edge of the Van Allen radiation zones. It is found, however, that the outer magnetosphere can be as difficult a region for spacecraft operation as are the lower altitude orbits. This difficulty comes about due to intense, hostile radiation environments of a transient nature. Three primary forms of radiation affect spacecraft system in the outer magnetosphere. There are:

1.   Solar flare particles

2.   Magnetospheric substorm particles

3.   Very high energy electrons

The damaging component of solar flare particles is primarily ions (mostly protons) of 10 to ~ 200 MeV kinetic energy. The second source, the magnetospheric substorm, produces large fluxes of low-to-moderate energy ions and electrons; the mechanism of damage is primarily one of surface and near-surface spacecraft charging effects. The very high energy electrons are 2-10 MeV in kinetic energy and their origin is at present uncertain.

Figure 1 shows the energy range of particles affecting spacecraft in the outer magnetosphere. In a typical transient substorm event, the magnetosphere produces ions and electrons up to a few hundred keV. (Occasionally bursts are observed up to ~ 1 MeV.) Most of the population above a few hundred keV shows enhancement due to processes occurring outside the magnetosphere. As shown by the cross-hatched shading, solar flares tend to produce large proton fluxes with $E \lesssim 200$ MeV; above this energy the particles are of low flux and are primarily galactic cosmic rays. As will be shown, the shaded parts of the spectrum in Fig. 1 are readily measured by the sensor systems being flown at 6.6 R_E today.

Fig. 1. Energetic Particle Spectrum in the Outer Terrestrial Magnetosphere Showing the Sources of the Particle Populations as Function of Energy.

The occurrence of operational problems for spacecraft can be viewed in two quite separate ways. One way is to try to predict when transient environmental effects will occur and to then take some sort of securing measures to prevent harmful consequences. Such an approach is possible in many cases, but predictions are not always accurate, and protective measures are not always possible. The second approach is to understand better the kinds of disturbances that occur in near-earth space and to design spacecraft to withstand such effects. Although this may increase construction cost and complexity, it is by far the preferred strategy for successful operation. It is our purpose here to demonstrate some of the known environmental effects associated with high-energy electrons and, also, to describe possible predictive methods that may be employed to deal with this deleterious component.

II. VERY HIGH ENERGY ELECTRONS AT ~ 6.6 R_E

The existence of populations of very high energy ($\gtrsim$ MeV) electrons deep in the earth's radiation belts have long been known.[1] These electrons constitute a primary integrated dose (fluence) problem for operation of spacecraft below ~ 4 R_E altitude as was noted before. It has been widely believed, however, that the intensity of such particles dropped off very rapidly with geocentric distance such that little flux remained beyond L ~ 5.

Unexplained anomalies in the performance of satellites often have occurred at synchronous altitude. Spacecraft surface charging has been implicated as a cause of some anomalies;[2] however, in other cases the penetrating radiation is clearly involved. In fact, satellite anomaly investigations precipitated a reconsideration of the model representing the trapped radiation environment.[3] Unfortunately, the population of electrons with energies much greater than 1 MeV had not been adequately characterized since such measurements require specialized instrumentation. In order to define better the populations of electrons at these high energies and their variations over long periods of time, a project was undertaken by the Los Alamos National Laboratory to develop an electron spectrometer which could make the required measurements.[4]

The new, high-energy electron measurements were made with an instrument called the Spectrometer for Energetic Electrons (SEE) which has been flown aboard several synchronous-orbit satellites. The data discussed in this report were acquired aboard S/C 1979-053 and S/C 1982-019. The spectrometer is a two-element telescope; it is illustrated schematically in Fig. 2. The silicon detectors provide a coincidence signal for the scintillation crystal made of BGO (bismuth germanate, $Bi_4Ge_3O_{12}$). The solid state detectors consist of two 1500 μ thick, ion-implanted Si elements for S/C 1979-053 and two 100 μ ruggedized, surface-barrier Si elements for S/C 1982-019. The BGO crystal measures the residual electron energy. Except for the 15° half-angle field-of-view, the detector is surrounded by a 5 gm/cm^2 aluminum shield which stops electrons with energy $\gtrsim$ 15 MeV.

PHOTOMULTIPLIER
TUBE ─╮   ╭─ LIGHT PIPE

$$G = 0.15 \ cm^2 - sr$$

BISMUTH GERMANATE
CRYSTAL $(Bi_4Ge_3O_{12})$ ─────
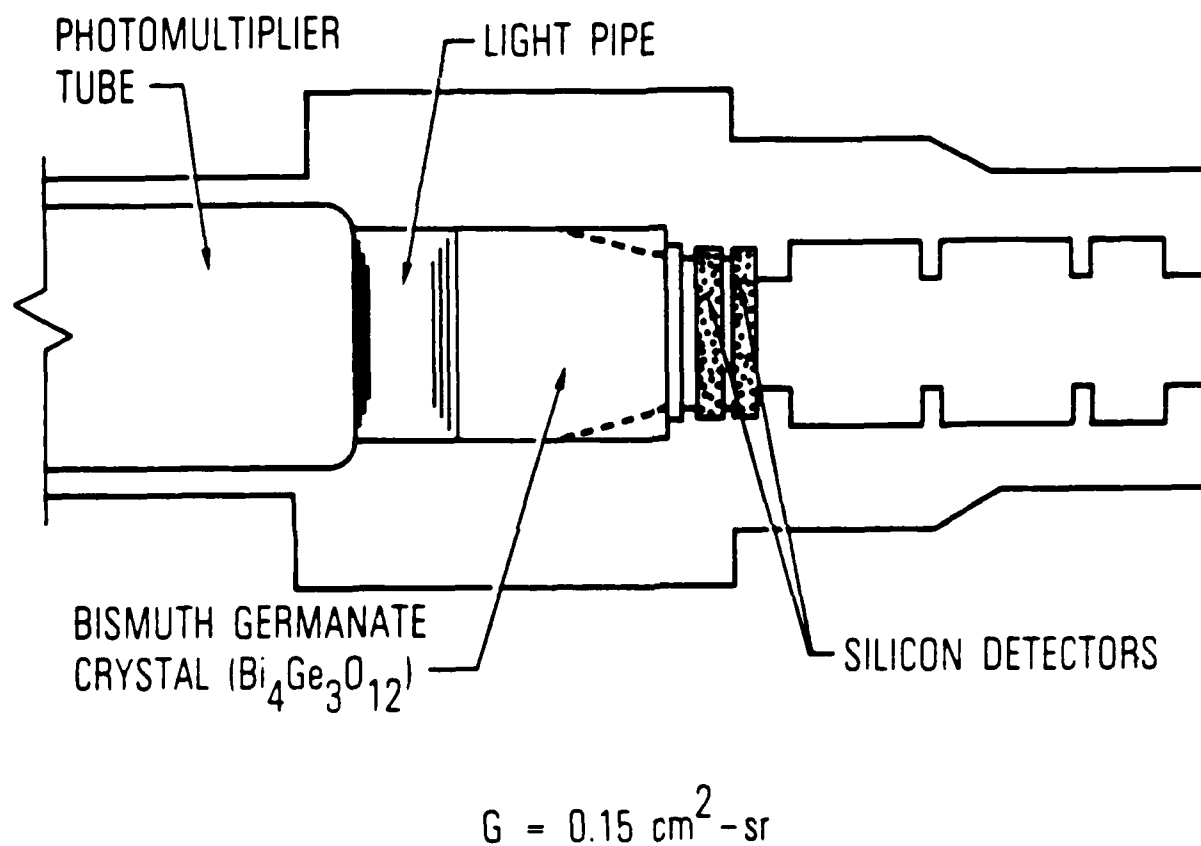
SILICON DETECTORS

Fig. 2.   Schematic Illustration (in Cross-Section) of the Spectrometer for
          Energetic Electrons (SEE). The essential features include the
          collimator structure to the right, the silicon solid-state detectors
          (operated in parallel), and the BGO analyzed crystal. The sensor
          has a geometric factor of 0.15 cm^2-sr; in addition to the illus-
          trated structure there is shielding of 0.34 g/cm^2 of Al in front of
          the collimator.

8

The BGO crystal is a cylinder 3.18 cm in diameter and 3.18 cm long. The silicon detectors are a stacked pair connected in parallel to the amplifier chain. Approximately 0.34 gm/cm^2 of aluminum (in the form of a slab) in the SEE field-of-view serves to reduce the single rates due to low-energy electrons and protons in the silicon detectors to acceptable values. The coincidence resolving time between the silicon and BGO detectors is ~1 μs. The gating window for electrons in the silicon detector goes from 0.90 to 1.5 MeV, which eliminates protons with energy ≤ 400 MeV which enter through the aperture from analysis. The BGO signals are pulse-height analyzed into five levels, thus providing four differential energy channels. The highest level serves to reject energetic protons except for a small percentage of particles that just cut the corner of the crystal. The BGO crystal in the second instrument is tapered (dotted lines in Fig. 2) to reduce this background component. Essentially all of the analyses that are presented in this report are based upon daily averages of SEE counting rates in the four SEE differential energy ranges: 3-5 MeV, 5-7 MeV, 7-10 MeV, and 10-15 MeV.

Figure 3 is a summary of SEE data showing the daily average of the count rates in the 3-5 MeV energy channel for the time period from June 1979 to the end of October 1984. The data are shown as the logarithm of counting rate versus day of year. The upper panel illustrates data from the instrument aboard S/C 1979-053, while the lower panel shows data in the same (lowest) energy channel of the instrument on board S/C 1982-019. No background or other corrections have been applied to the data.

The intensity variations in Fig. 3 show many of the same characteristics observed previously in the Charged-Particle Analyzer (CPA) data.[5] Numerous narrow intensity peaks are observed and these are separated by broad count rate minima. Careful examination of the data (e.g., in late-1980 and early-1981) shows flux peaks which are ~ 27 days apart as was found earlier.[5]

A substantial difference in peak particle count rates is found in the data obtained prior to 1981 and those obtained after the beginning of 1981. In Fig. 3 notice that in 1979 and 1980 there was only one event (June 1980) in
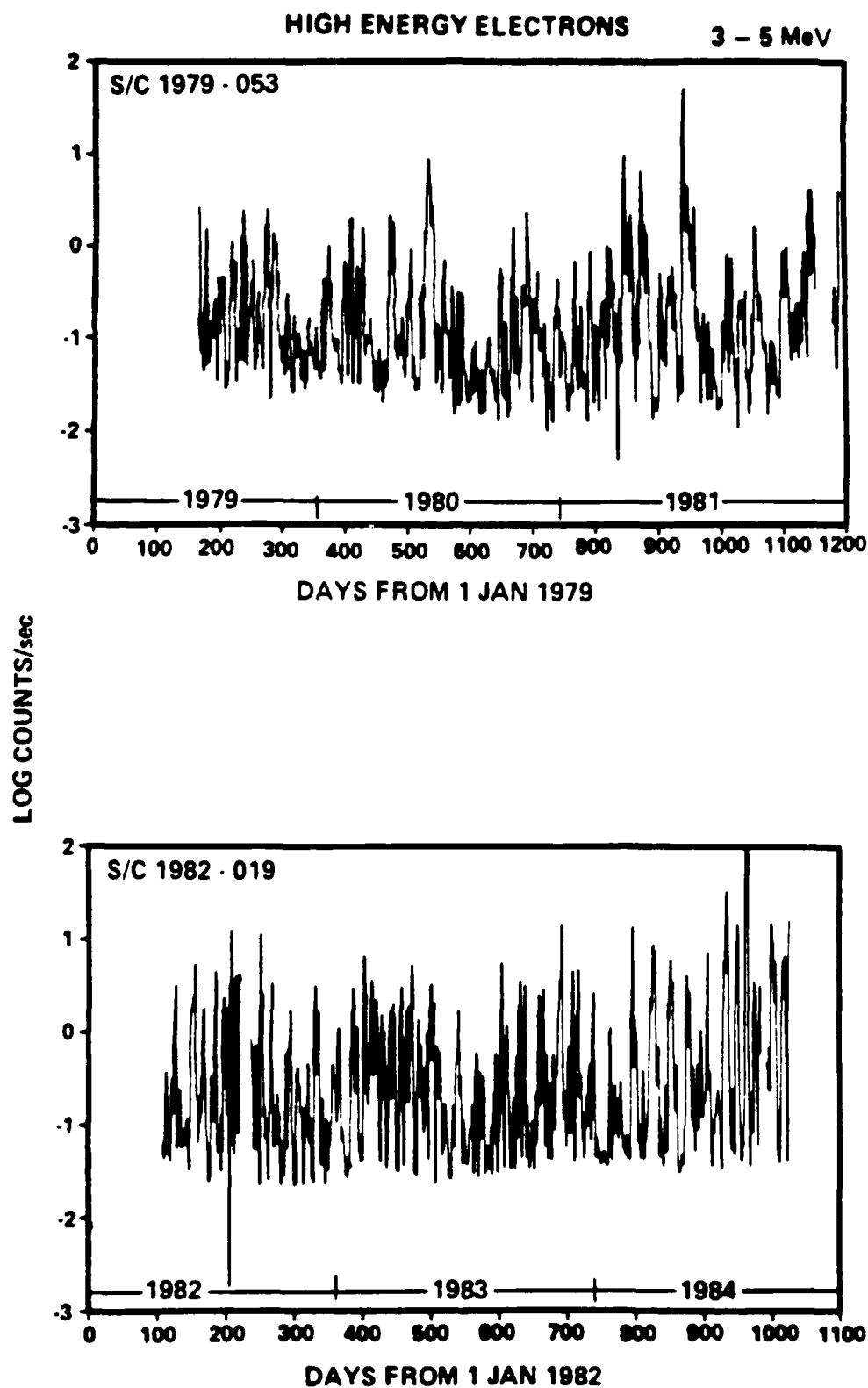
Fig. 3.   High-Energy Electron (3-5 MeV) Daily Count Rate Averages from June
1979 through October 1984. Data are from nearly identical instru-
ments onboard spacecraft 1979-053 (upper panel) and spacecraft 1982-
019 (lower panel).

10

which the 3-5 MeV count rate substantially exceeded ~ 3 counts/sec. Beginning in 1981, and throughout the remainder of the data set, peak counting rates very commonly exceeded 3 counts/sec and often were much higher. Thus, a general result obtained from the data is that, on average, 3-5 MeV fluxes were much higher at 6.6 R_E in 1982-84 than in 1979-80.

This result is more clearly demonstrated by examination of the 5-7 MeV data, shown in Fig. 4. Note the strong contrast in Fig. 4 between the count rate profile prior to 1981 and afterwards. Except for the period of the June 1980 event, there were only small, weak flux increases in the 5-7 MeV energy range. In contrast, beginning in 1981, numerous large flux increases were seen and continued to occur into 1984 when the presently analyzed data set ends.

Two other features of the observations are well illustrated by Fig. 4. First notice the smooth, systematic variation of the minimum count rates seen in the 5-7 MeV channel. This minimum count rate, which we attribute to background, was relatively high and steady at ~ 0.03 counts/sec in 1979 and early 1980. It then diminished rapidly in late 1980 and 1981, with a recovery by early 1982. Another deeper minimum in the SEE background was seen in later 1982 with a gradual recovery to ~ 0.02-0.03 counts/sec by 1984. This time dependence of the background in the SEE sensor is the same as the average Deep River Neutron Monitor count rate.[6] The neutron monitor data are a measure of the intensity of several hundred MeV/nucleon cosmic rays and are the major source of background for the SEE instrument as discussed above. We have drawn the smoothed cosmic ray background[6] profile in Fig. 4 as a dashed line.

A second clear feature of the data plotted in Fig. 4 is the often highly periodic occurrence of large count rate enhancements. This effect was very evident in the 1982-84 time period. In the lower panel of this figure we have shown a small inset with 27-day tick marks referenced to a large event (see the asterisk) which occurred in July 1984. At least six, and perhaps as many as a dozen, flux peaks are seen to be separated by periods which occur modulo 27 days, the synodic period of the sun.
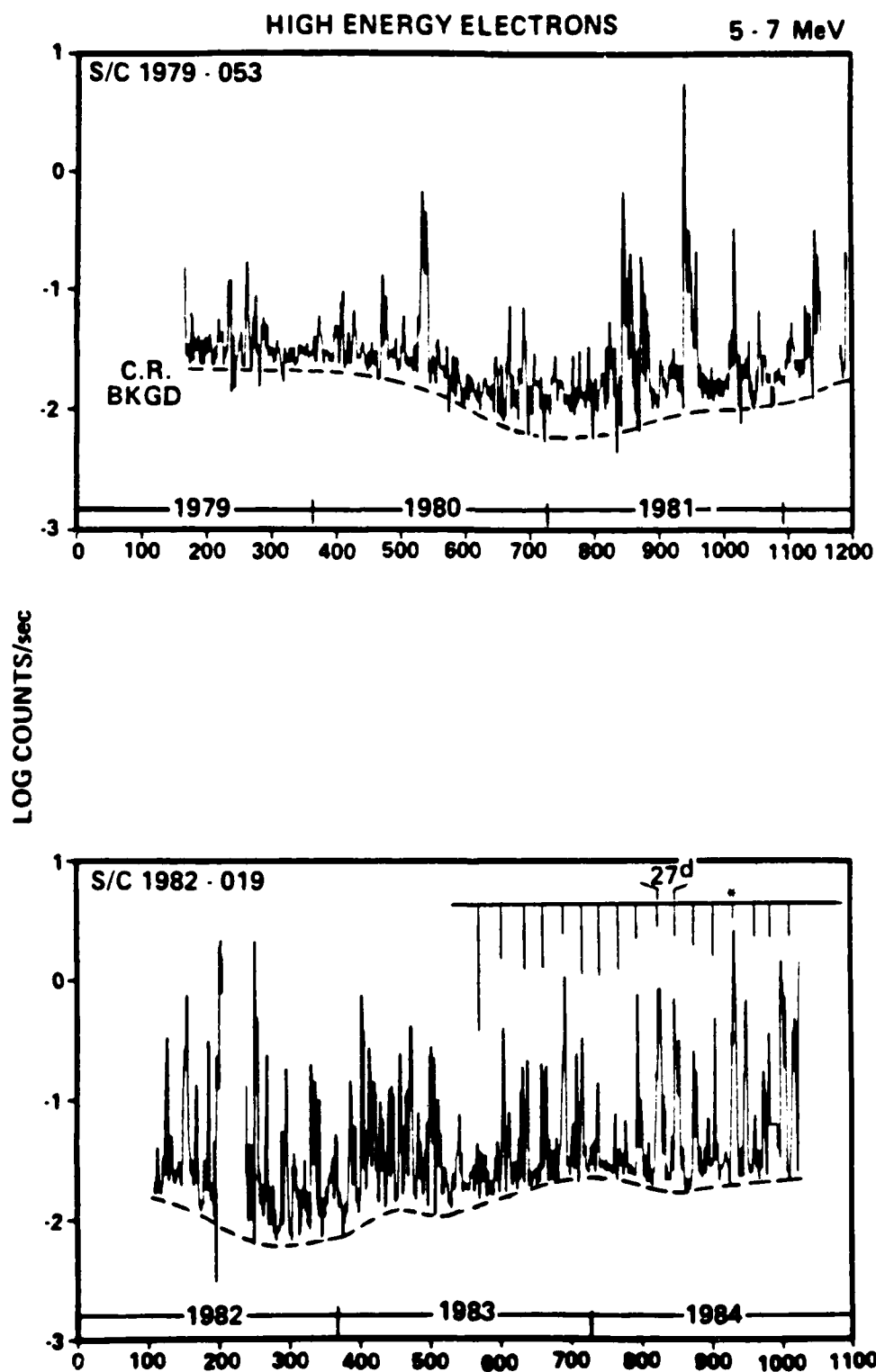
11

Fig. 4.   High-Energy Electron (5-7 MeV) Daily Count Rate Averages from June
1979 through October 1984. Note the periodic intensity enhancements
illustrated by the inset in the lower panel.

12

Figure 5 shows a variety of data from June 1980. Recall from Figs. 3 and 4 that this time period included one of the largest electron enhancements seen by the SEE sensors around solar maximum. In the figure we show data from 10 June to 20 June 1980. The top panel shows the geomagnetic storm index, Dst, at 1-hr resolution (solar-geophysical data). In the second panel we show the 3-hr planetary activity index, Kp. The third panel shows the 7-10 MeV electron fluxes in the form of daily averages. Finally, the fourth panel shows the solar wind speed as measured by ISEE-3 in the form of 3-hr averages.

The patterns seen in Fig. 5 agree very well with those reported previously by Paulikas and Blake[7,8] and Baker et al.[5] Geomagnetic storm activity was seen on 10 June through 13 June 1980 as indicated by large, negative values of Dst and by high Kp levels. This geomagnetic activity was produced by a high-speed solar wind stream ($V \gtrsim 600$ km/s) and by associated solar wind density and magnetic field conditions. The large increases in relativistic electrons observed by the SEE detector at 6.6 R_E began after ~ 12 June as Kp and Dst were returning to quiet levels and as the solar wind speed rapidly diminished.

The occurrence of very high energy electrons at 6.6 R_E is of substantial practical importance and interest. We have found numerous examples of spacecraft operational problems occurring during such flux enhancements. An example of such a recent event is shown in Fig. 6. The figure shows daily average counting rates at two energy levels: 3-5 MeV and 5-7.5 MeV. Data are shown for the middle period of July 1984. Note that background levels for the sensor (determined largely by galactic cosmic rays) are at ~ 0.05 c/s.

A long-lasting and relatively symmetric increase of electron fluxes began on 14 July. Over the succeeding week the intensities increased by ~ 3 orders of magnitude in the 3-5 MeV channel. Highest fluxes were observed on 21 July after which a relatively rapid flux decrease occurred at all energies. This event was the largest observed (by a factor of ~ 3) in the first 2.5 years of operation of the spacecraft.
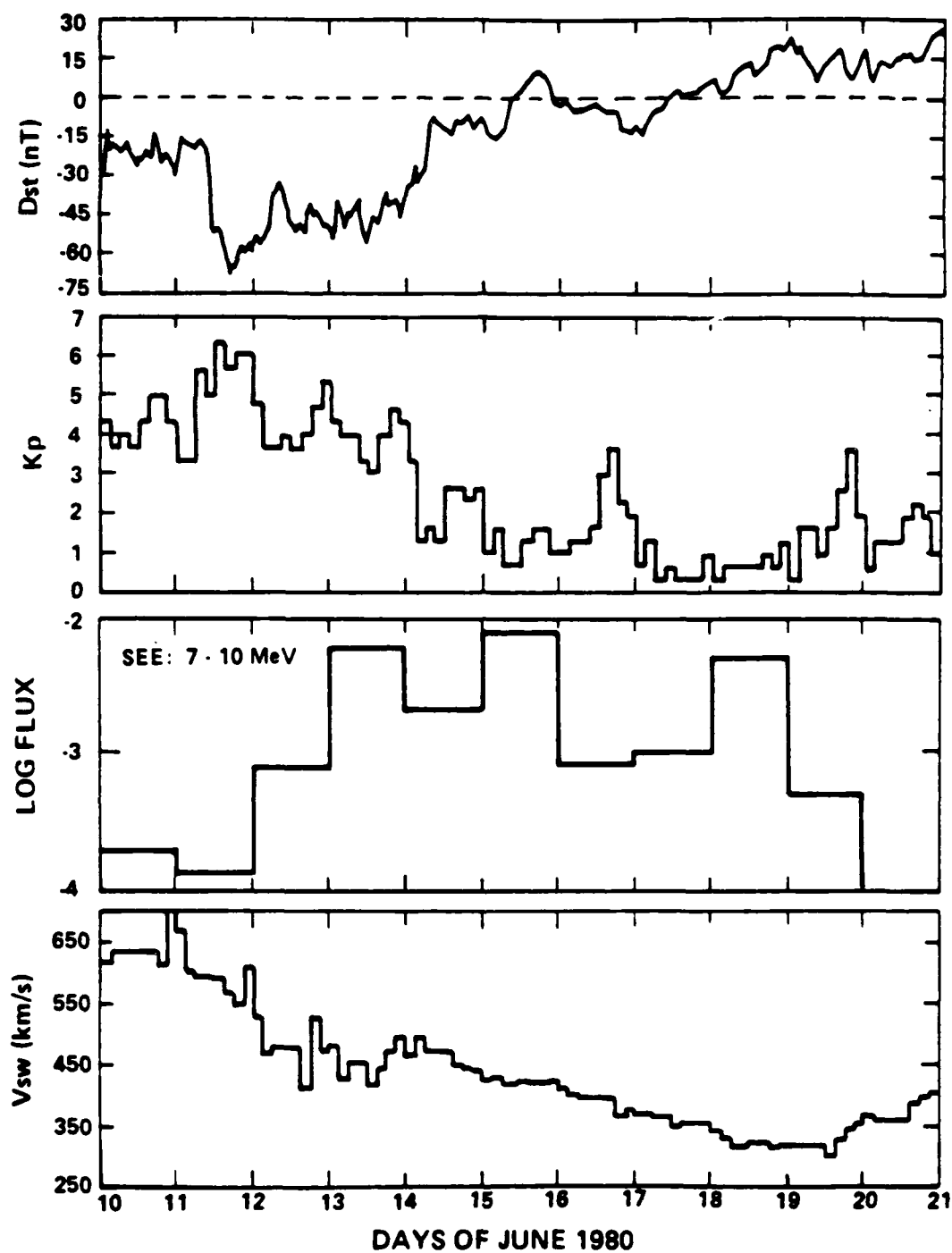
Fig. 5.   Several Data Sets (as Discussed in the Text) for a Period in June
1980 During Which a Large SEE Electron Event was Observed. The SEE
flux enhancement (3rd panel) occurred as Dst, K_p, and the solar wind
speed (V_{sw}) recovered following a geomagnetic storm.

14
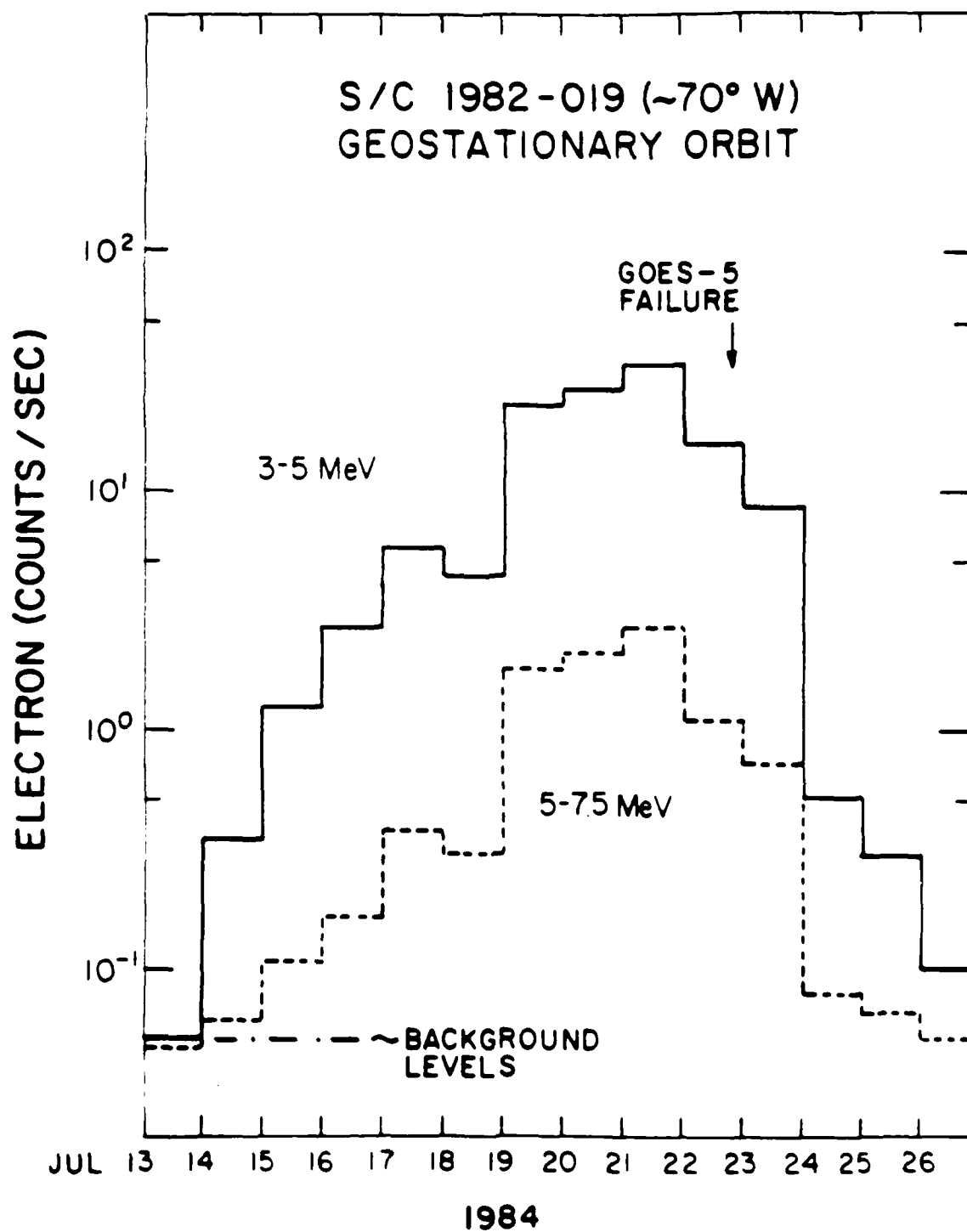
Fig. 6.   Detailed Plot of Very Energetic Electron count Rates at 6.6 R_E in Two Energy Ranges for a Two-Week Interval in July 1984. During this very intense event, GOES-5 experienced a hardware failure.

Late on 22 July 1984, while energetic electron fluxes were still very high at 6.6 R_E, GOES-5 experienced the failure of a filament in an encoder lamp (J. H. Allen, private communication). This failure greatly compromised the GOES-5 capability for providing weather images for the eastern U. S. The mechanism by which relatively low absolute numbers of high energy electrons could produce a failure in a tungsten encoder lamp may involve "deep-charging" effects as we will discuss below. The occurrence of the failure during a particularly strong electron event, in fact, suggests that the high energy electron component is involved.

Another class of anomalies for which the high energy electron component is clearly implicated is shown in Fig. 7. These data are an expanded subset of data shown in Fig. 3. Intensities of 3 MeV electrons are illustrated from approximately October 1980 to early April 1982.

During this broad interval of time, the star tracker system onboard the geosynchronous satellite experienced repeated upsets. The times of star tracker upsets are shown by the short vertical arrows. Some notable features are immediately evident from the figure. First, the upsets occurred essentially whenever fluxes of electrons exceeded an approximate empirical level of 6 count rate units. Secondly, the disruptions never were seen when fluxes remained below this empirical level. The high degree of correlation between these sensor upsets and very energetic electrons fluxes is strong evidence for a causal relationship between the environment and the anomalies.

The problem manifested in the example of Fig. 7 seems to be an electronic disruption in a solid-state detector control circuit. It has been shown[9] that irradiation of space systems by very energetic electrons can cause a deep dielectric charging phenomenon. Essentially, very high energy electrons can bury themselves in dielectric materials (e.g., coaxial cables, etc.) and stop. They then give rise to very high electric fields (potential differences of several kilovolts) in these regions until eventually an intense breakdown occurs. Hence, in the example of Fig. 7 a very strong correlation of spacecraft ancmalies with the environment exists and, further, a plausible physical connection can be established.
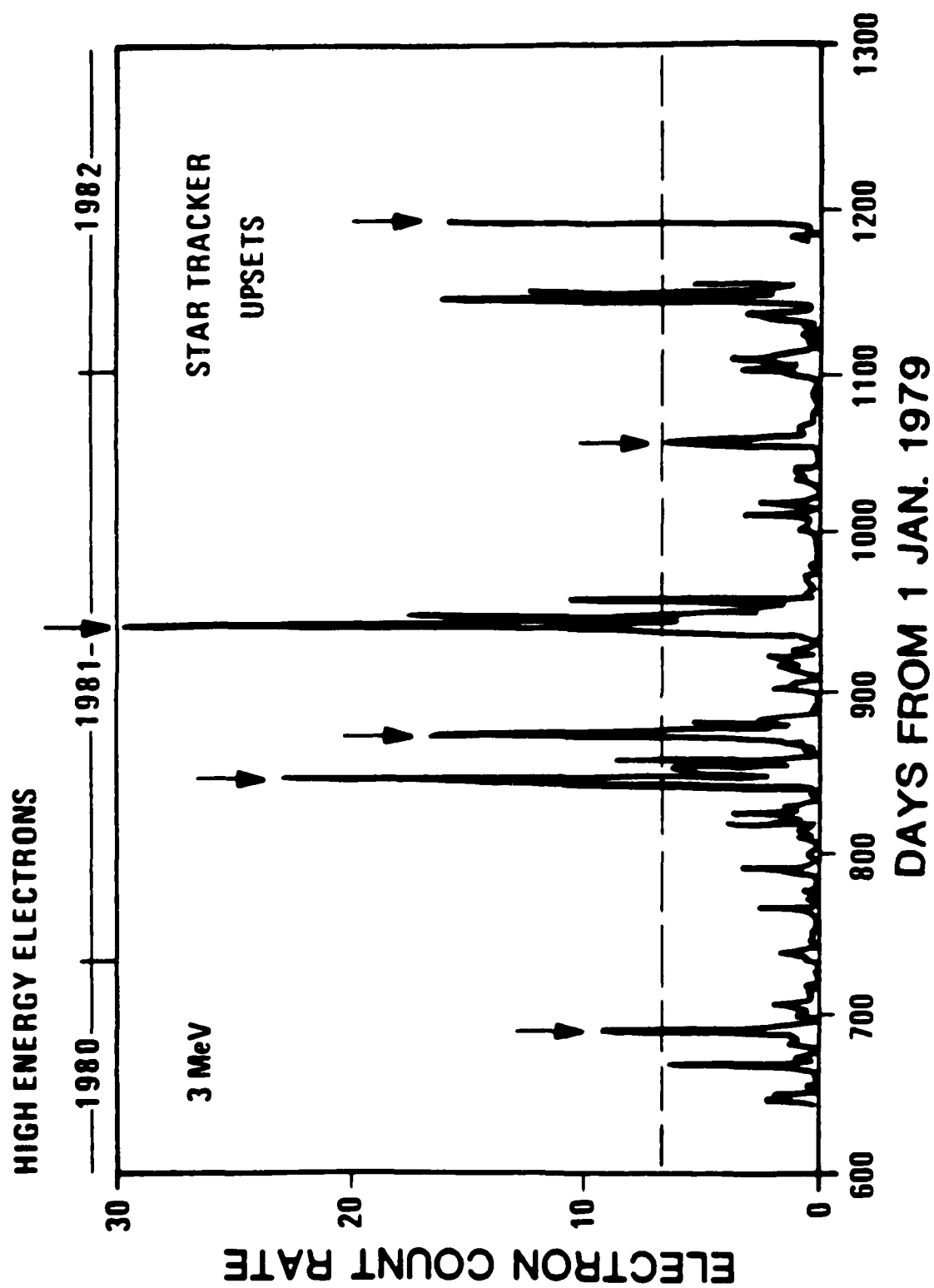
16

Fig. 7. Detail of Data in Fig. 3 Showing the Relationship of Star Tracker Anomaly Intervals (Vertical Arrows) with the Occurrence of Intense Electron Events.

Unfortunately, it is very difficult to shield against multi-MeV electrons. The greatest hope is to be aware that such particles occur rather regularly at 6.6 R_E and to design systems and subsystems which are immune to their effects. From the standpoint of predictions, we are finding considerable evidence that this very energetic component recurs with a regular 27-day (solar rotation) periodicity,[4,5] and thus we should eventually be able to predict the times of their occurrence reasonably well.

The discussion of the relativistic electron flux increases so far has been mainly in terms of temporal variations; it also is of interest to examine the spectral variations of the electron population. In an effort to understand how the intensities of relativistic electrons relate to lower-energy populations, we have examined many events in detail. Figure 8 shows a plot of the electron energy spectra for selected days during the June 1980 event discussed above. The spectra combine data from the CPA high energy (0.2-2.0 MeV) system with the data from the SEE detector system on the same geostationary spacecraft. For reference the spectra given by the two NASA electron models, AE-7HI and AE-8Max, are shown. The models show a spectral truncation at several MeV whereas the SEE measurements exhibit no truncation and even show a spectral hardening at higher energies; the observed daily average fluxes in the large June 1980 event follow a hard exponential spectrum up to at least 10 MeV. It is clear that the NASA models,[1] although they correspond quite well to the measurements at energies below ~ 1 MeV, do not correctly describe the environment above a few MeV. Most of the other periods of substantial energetic electron fluxes identifiable in Figs. 3 and 4 show spectral relationships similar to those illustrated in Fig. 8.

We have performed a superposed epoch analysis of all available SEE data to characterize the lifetimes of the relativistic electron populations. The analysis consisted of the following steps:

1. All peaks seen in Channel 1 (3-5 MeV) with a peak count rate ≥ 3/sec were tabulated.

2. The day-of-maximum for each such peak was determined, and was designated T_o.
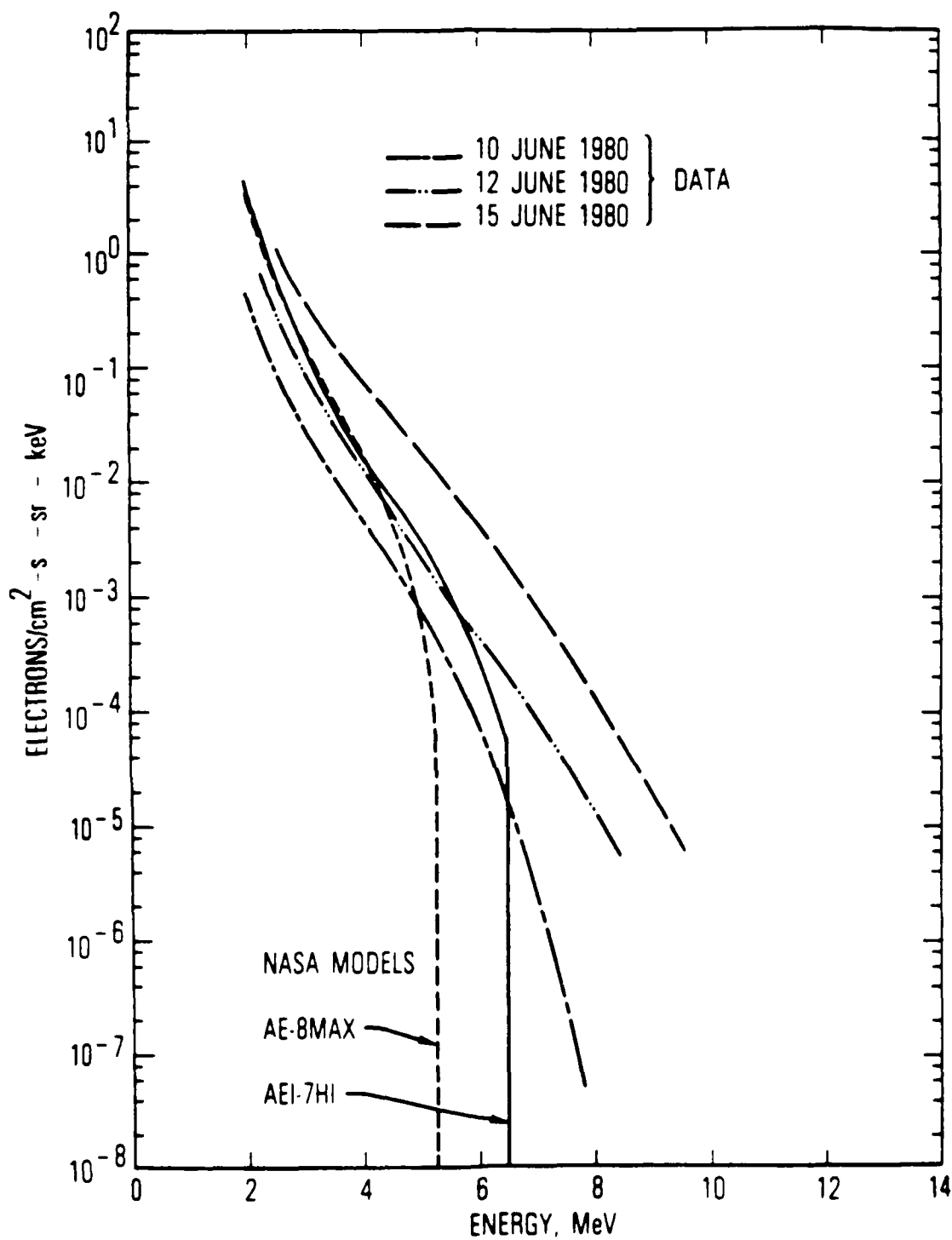
18

Fig. 8. A Comparison of Measured Electron Energy Spectra Obtained by Sensors Onboard S/C 1979-053 at 6.6 R_E (in June 1980) with two NASA Environmental Models for that Region of Space. Note that the NASA models are truncated in energy, while the measured spectra remain relatively hard exponentials as high as 10 MeV.

19

3. Data were grouped from T_0 - 6 days to T_0 + 15 days to form an event interval.

4. The count rates for the 3-5 MeV channel were normalized to the peak rate at T_0 for each interval (but the 5-7 MeV count rates were separately normalized to the maximum count rate for that energy, irrespective of which day it occurred on).

5. The normalized count rates were plotted together to produce epoch flux profiles for a given channel.

Figure 9 summarizes this epoch analysis for the 3-5 MeV (upper panel) and the 5-7 MeV (lower panel) data from S/C 1979-053. In our analysis we used the same epoch intervals for Channel 2 that were used for Channel 1. In principle the Channel 2 profiles could peak at any day number and certainly need not peak at Day 0. Note in the figure, however, that the Channel 2 data show a strong tendency to also peak on Day 0. Thus, no significant differences of occurrence time or lifetime are found as a function of energy for this popula-tion. The results of Fig. 9 show that an average event (in the 3-5 MeV range) rises out of the background level 2-3 days before the time of peak intensity and decays back to approximately this same level on a similar time scale. Other than the higher average background rate, the 5-7 MeV results in Fig. 9b are nearly identical to the results of Fig. 9a. A full-width at half-maximum for an average event is ~ 2-5 days.

To test the generality of these results, we analyzed data from S/C 1982-019 separately. The results of these analyses, using an identical approach to that described above for S/C 1979-053, are shown in Fig. 10. Notice that the average relative background rates both for Channel 1 and Channel 2 are much smaller due to much more distinct peaks seen in the flux profiles (Figs. 3 and 4) during 1982 through 1984. The results for S/C 1982-019 (using data from 1982-84) are, nonetheless, essentially the same as those obtained from S/C 1979-053 from 1979 to 1982. Thus, we conclude that average particle life-times, rise and decay time scales, and all relevant physics involved in these effects seem invariant as a function of time within the solar cycle.

AVERAGE EPOCH ANALYSIS OF SEE DATA

CHANNEL 1 (3 – 5 MeV)

CHANNEL 2 (5 – 7 MeV)

Fig. 9. Superposed Epoch Analysis (as Described in the Text) for 3-5 MeV
(Upper Panel) and 5-7 MeV (Lower Panel) Electrons Measured by the
SEE Sensor System on S/C 1979-053 from June 1979 to April 1982.
Note that a typical event peaks strongly at day 0 both in Channel 1
and Channel 2. In both cases, a typical event is ~ 2.5 days wide
(FWHM).

AVERAGE EPOCH ANALYSIS OF SEE DATA

CHANNEL 1 (3 – 5 MeV)

S/C 1982 · 019

CHANNEL 2 (5 – 7 MeV)
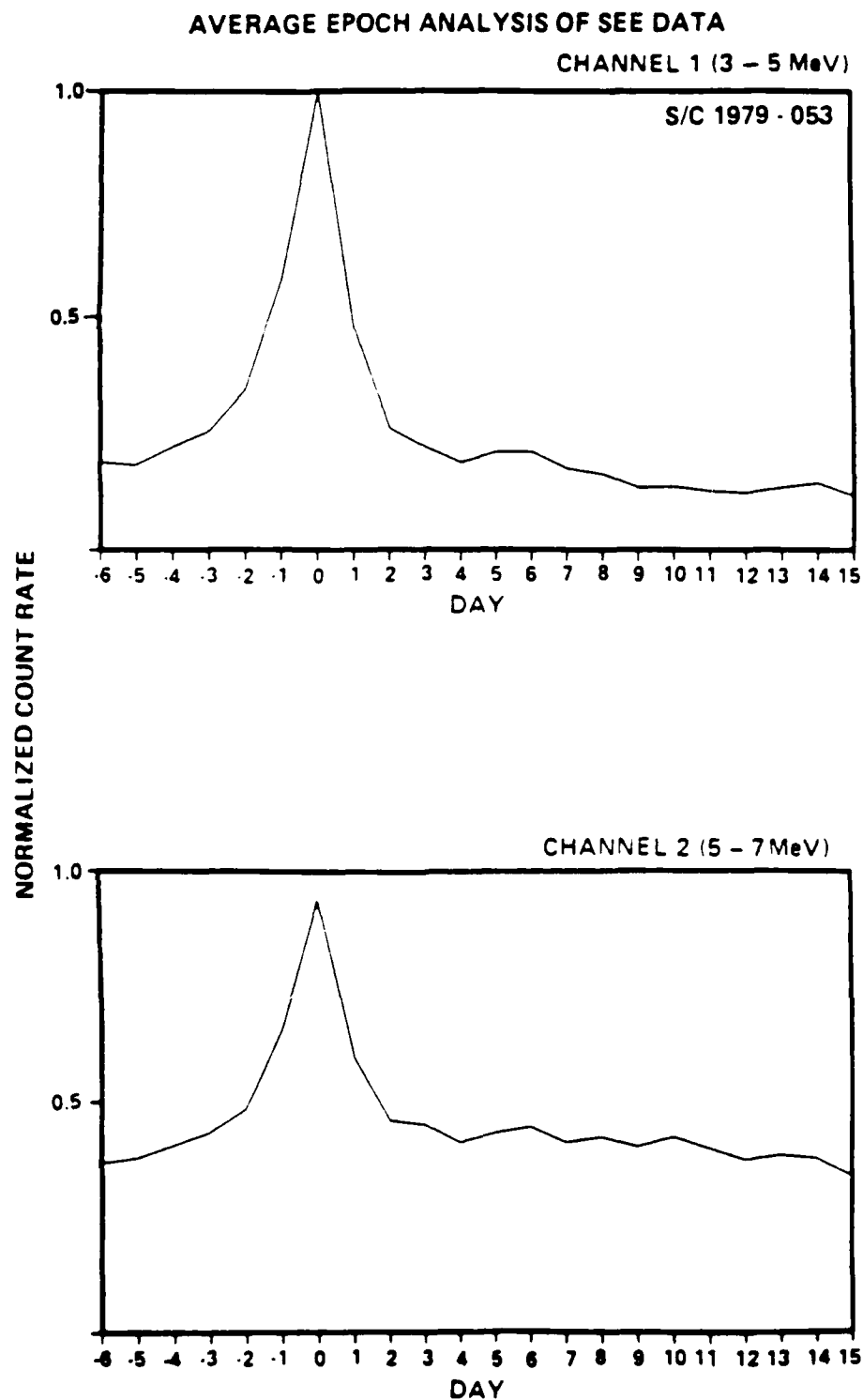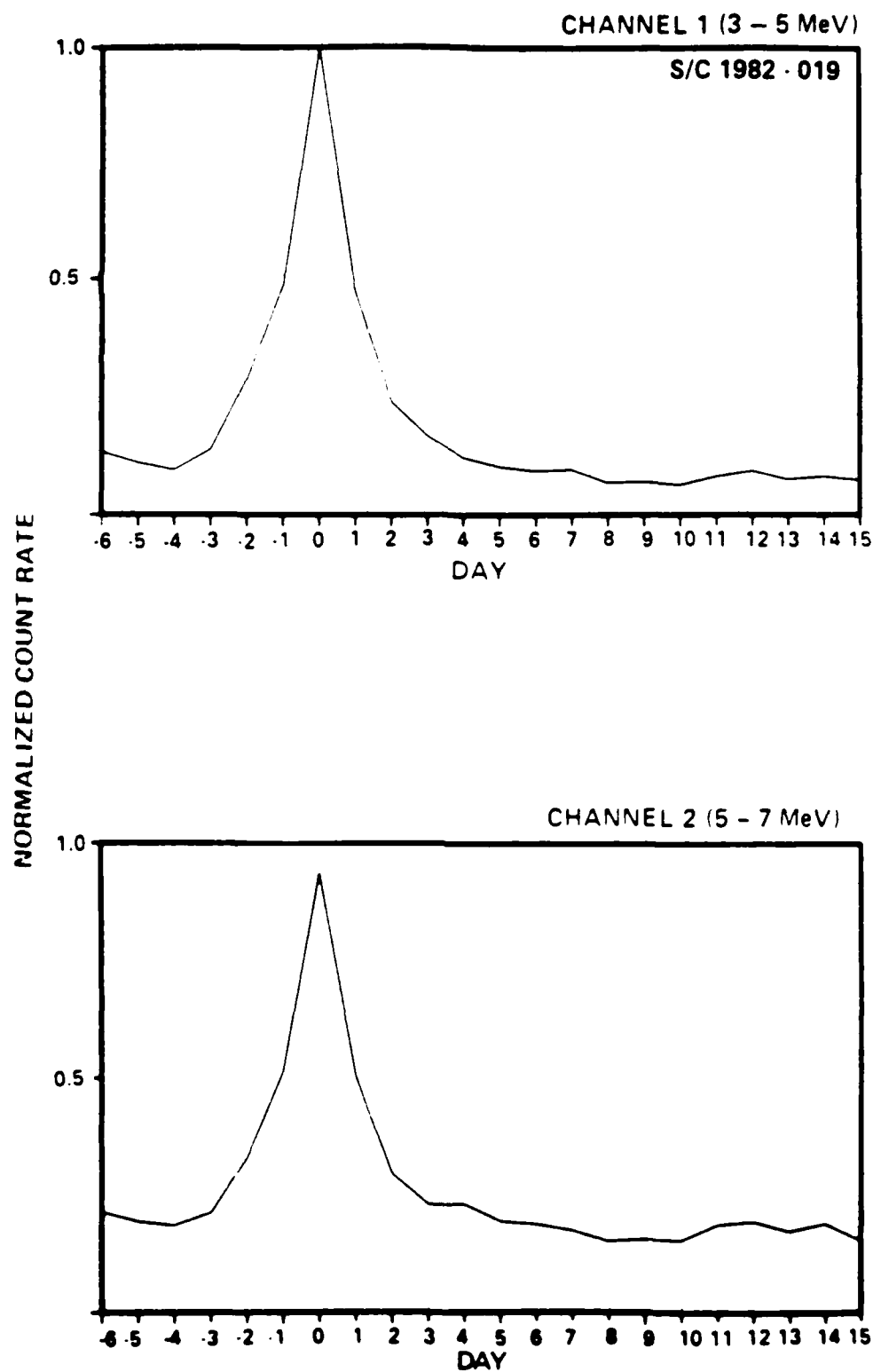
Fig. 10. Superposed Epoch Analysis for 3-5 MeV (Upper Panel) and 5-7 MeV (Lower Panel) Electrons Measured by the SEE Sensor System on S/C 1982-019 During the Period 1982-1984.

22

III. DISCUSSION

No systematic observations of electron fluxes and energy spectra in the outer terrestrial magnetosphere have previously been available at energies up to 15 MeV. The present measurements therefore give us a new perspective on an important component of the trapped radiation environment. The main observational results are as follows:

1. In support of previous observations at lower energy, the trapped electron population in the outer terrestrial magnetosphere often exhibits large flux enhancements up to $E \geq 10$ MeV.

2. Around solar maximum (1979-80) there were very few large electron flux increases in the > 3 MeV population at 6.6 R_E.

3. During the declining phase of solar cycle 21 (1981-1984), there were large and frequent increases in the highly relativistic electron fluxes at 6.6 R_E.

4. The increases in the multi-MeV electron fluxes often exhibit a very regular 27-day periodicity which seem well-associated with recurrent solar wind stream structures.

5. Superposed epoch analysis shows that these electron fluxes, on average, rise on 2-3 day timescales, reach a maximum, and decay back to prior levels on 3-4 day timescales. Full-width at half-maximum timescales for typical events are ~ 2.5 days.

We have stated above that the highly variable relativisitic electron component at 6.6 R_E is trapped; this follows directly from consideration of the relatively low rigidity of these particles (implying that they cannot penetrate directly from beyond the magnetopause to 6.6 R_E) and from the strong diurnal variations we observed (due to adiabatic drift in the terrestrial magnetic field). Two primary models have been suggested for this component: the internal magnetospheric generation model and the external source model, with the initial acceleration occurring either at Jupiter or the Sun.

The internal generation model was first suggested by Paulikas and Blake[8] as an interpretation of energetic electron results from ATS-6. They argued that increased solar wind speed produced stronger and more frequent magnetospheric substorm activity and greatly enhanced radial diffusion. One of the

23

prompt products of such substorm activity is high fluxes of relatively low-energy ($\lesssim$ 1 MeV) electrons. A magnetospheric mechanism then processes this population of electrons for some days, creating a steadily increasing population of several MeV electrons at geostationary orbit. The second step of the acceleration process involved is attributed, for want of a better explanation, to radial diffusion; as electrons diffuse inward to smaller and smaller L-shells, conserving their first and second invariants, they gain appreciable energy.[10] Electrons thus energized by inward radial diffusion to L $\sim$ 3-4 somehow return to L = 6.6, perhaps by the mechanism discussed by Nishida,[11] largely preserving the energy that they gained in the inward diffusion process.

An alternative model was suggested by Baker et al.[5] Jovian electrons, controlled by solar-wind stream structure, regularly appear in the vicinity of the earth.[12,13] Jovian electrons are observed down to energies at least as low as 200 keV, and these electrons presumably can enter the distant plasma sheet essentially unattenuated. This Jovian population then could merge with the plasma sheet population and begin to participate in the overall magnetospheric dynamics. During earthward convection the plasma sheet population, including the Jovian electrons, is swept nearer the earth and during substorms convected even more strongly and injected into the synchronous-orbit region.

Analysis continues as to whether the internal generation model, the external source model, or both are responsible for the high energy electrons at 6.6 R_E.

IV. CONCLUSION

The increasing complexity and capability of modern space systems has been remarkable. We may expect even more extensive use of very large-scale integrated circuits (VLSI) in space, and we may also expect faster and more powerful processors, controllers, and memories to be employed. Unfortunately, as capabilities of electronics go up, the susceptibility to radiation effects also goes up. This point is made in Fig. 11. In the lower portion of the figure we show a schematic of the decreasing "hardness" of electronic components in space. This can be hardness to charging effects, or radiation damage, or other environmental factors. In any case this hardness is diminishing and, we fully expect, will continue to do so. Even if this were not true at the component level, the increasing complexity would still put the overall system functions at risk.

The upper part of Fig. 11 shows some of the variations we expect in the solar-terrestrial environment. We can expect that every 11 years there will be an increase and decrease of solar activity as measured by sunspot number. In rough synchronism with this cycle we can expect to see large numbers of solar flares and the concomitant solar particle events. In antiphase with solar activity we expect to see strong solar wind streams which drive strong, recurrent substorms and very energetic electron enhancements at 6.6 R_E.

The point of Fig. 11 is that with a certain kind of environmental sensitivity, a given spacecraft design may have a few "good years" (say near solar minimum or possibly near solar maximum). But then, immutably and predictably, the solar-terrestrial conditions will change and the environmentally unfavorable conditions will return. Designers of spacecraft should recognize that there are harmful elements of the solar-terrestrial environment and that they should consider this in their planning. They should also realize explicitly the kinds of periodicities that are an inescapable element of the solar-terrestrial system.
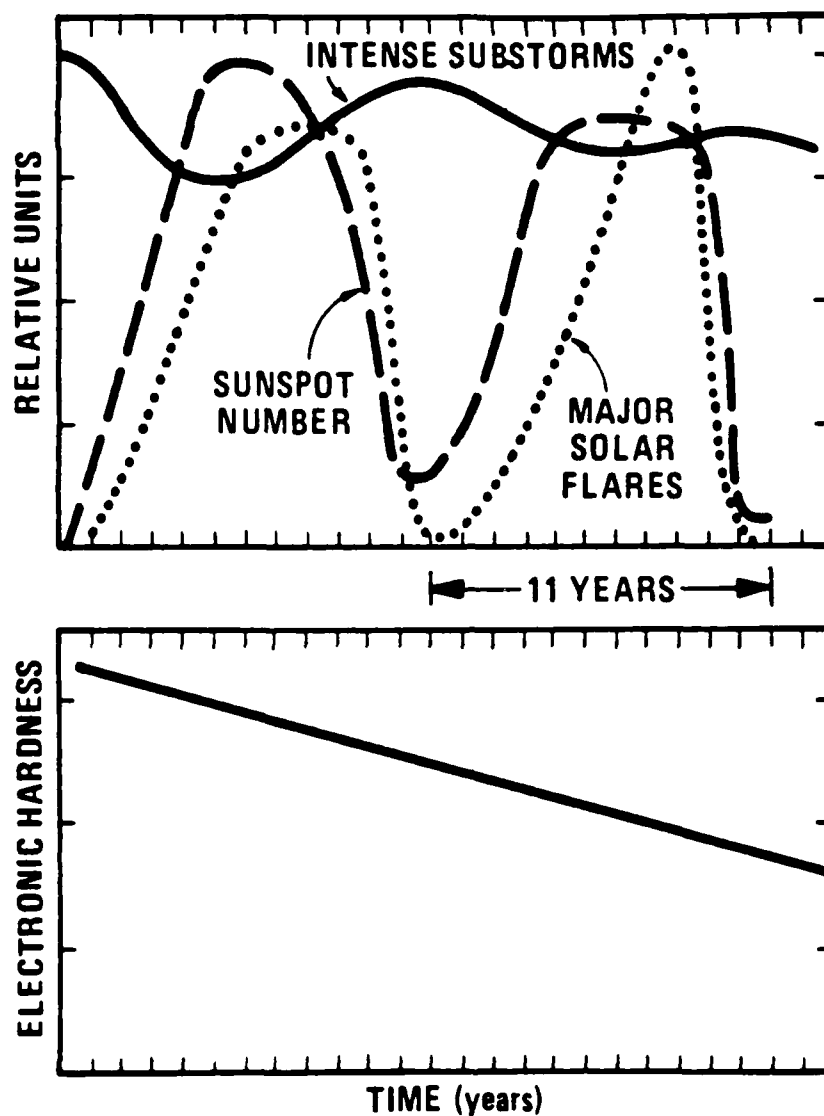
Fig. 11. Top panel: Some of the Known Long-term Periodicities in Solar and Geomagnetic Activity Which Should be Considered in Spacecraft Operations. Bottom Panel: A Qualitative, but Dangerous, Trend in the "Hardness" of Space Electronics to Radiation in Space.

As we have indicated previously, we are coming to an increasingly thorough understanding of the near-earth space environment. This theoretical understanding is sufficient that we even have a significant predictive capability. When possible we should use these abilities to forecast environmental conditions in space. In the long term, however, we are best advised, where possible, to recognize and understand the solar-terrestrial environment for what it is and thereby design our systems to withstand the rigors of operation in space. This seems especially true of the high-energy electron component discussed in this report.

REFERENCES

1. J. I. Vette, M. J. Teague, D. M. Sawyer, and K. W. Chan, "Modeling the Earth's Radiation Belts," In: R. R. Donnelly (Ed.), Solar-Terrestrial Predictions Proceedings, Vol. II, Boulder (1979) p. 21.

2. A. Rosen (Ed.) in: Spacecraft Charging by Magnetospheric Plasma, AIAA, Vol. 47, New York, (1976).

3. A. L. Vampola, J. B. Blake, and G. A. Paulikas, "A New Study of the Magnetospheric Electron Environment," J. Spacecraft Rockets, 14, 690 (1977).

4. D. N. Baker, J. B. Blake, R. W. Klebesadel, and P. R. Higbie, "Highly Relativistic Electrons in the Earth's Outer Magnetosphere, I. Lifetimes and temporal history 1979-84," J. Geophys. Res., 91 (1986).

5. D. N. Baker, P. R. Higbie, R. D. Belian, and E. W. Hones, Jr., "Do Jovian Electrons Influence the Terrestrial Outer Radiation Zone?" Geophys. Res. Lett, 6, 531 (1979).

6. R. W. Fillius and W. I. Axford, "Large Scale Solar Modulation of ≳ 500 MeV/n Galactic Cosmic Rays Seen from 1-30 AU, J. Geophys. Res., 90, 517 (1985).

7. G. A. Paulikas, and J. B. Blake, "Modulation of Trapped Energetic Electrons at 6.6 R_E by the Direction of the Interplanetary Magnetic Field," Geophys. Res. Lett., 3, 277 (1976).

8. G. A. Paulikas, and J. B. Blake, "Effects of the Solar Wind of Magnetospheric Dynamics: Energetic Electrons at the Synchronous Orbit," in Quantitative Modelling of Magnetospheric Processes, 21, Geophys. Monog. Series 180 (1979).

9. J. B. Reagan, R. E. Meyerott, E. E. Gaines, R. W. Nightingale, P. C. Filbert, and W. L. Imhof, "Space Charging Currents and Their Effects on Spacecraft Systems," IEEE Trans. Elec. Ins., EI-18, 354 (1983).

10. M. Schulz, and L. J. Lanzerotti, Particle Diffusion in the Radiation Belts, Springer, New York (1974).

11. A. Nishida, "Outward diffusion of energetic particles from the Jovian Radiation Belt," J. Geophys. Res., 81, 1771 (1976).

12. B. F. Teegarden, F. B. McDonald, J. H. Trainor, W. R. Webber, and E. C. Roelof, "Interplanetary MeV Electrons of Jovian Origin, J. Geophys. Res., 79, 3615 (1974).

13. T. F. Conlon, The Interplanetary Modulation and Transport of Jovian Electrons, J. Geophys. Res., 83, 541 (1978).

LABORATORY OPERATIONS

The Aerospace Corporation functions as an "architect-engineer" for national security projects, specializing in advanced military space systems. Providing research support, the corporation's Laboratory Operations conducts experimental and theoretical investigations that focus on the application of scientific and technical advances to such systems. Vital to the success of these investigations is the technical staff's wide-ranging expertise and its ability to stay current with new developments. This expertise is enhanced by a research program aimed at dealing with the many problems associated with rapidly evolving space systems. Contributing their capabilities to the research effort are these individual laboratories:

Aerophysics Laboratory: Launch vehicle and reentry fluid mechanics, heat transfer and flight dynamics; chemical and electric propulsion, propellant chemistry, chemical dynamics, environmental chemistry, trace detection; spacecraft structural mechanics, contamination, thermal and structural control; high temperature thermomechanics, gas kinetics and radiation; cw and pulsed chemical and excimer laser development including chemical kinetics, spectroscopy, optical resonators, beam control, atmospheric propagation, laser effects and countermeasures.

Chemistry and Physics Laboratory: Atmospheric chemical reactions, atmospheric optics, light scattering, state-specific chemical reactions and radiative signatures of missile plumes, sensor out-of-field-of-view rejection, applied laser spectroscopy, laser chemistry, laser optoelectronics, solar cell physics, battery electrochemistry, space vacuum and radiation effects on materials, lubrication and surface phenomena, thermionic emission, photosensitive materials and detectors, atomic frequency standards, and environmental chemistry.

Computer Science Laboratory: Program verification, program translation, performance-sensitive system design, distributed architectures for spaceborne computers, fault-tolerant computer systems, artificial intelligence, microelectronics applications, communication protocols, and computer security.

Electronics Research Laboratory: Microelectronics, solid-state device physics, compound semiconductors, radiation hardening; electro-optics, quantum electronics, solid-state lasers, optical propagation and communications; microwave semiconductor devices, microwave/millimeter wave measurements, diagnostics and radiometry, microwave/millimeter wave thermionic devices; atomic time and frequency standards; antennas, rf systems, electromagnetic propagation phenomena, space communication systems.

Materials Sciences Laboratory: Development of new materials: metals, alloys, ceramics, polymers and their composites, and new forms of carbon; nondestructive evaluation, component failure analysis and reliability; fracture mechanics and stress corrosion; analysis and evaluation of materials at cryogenic and elevated temperatures as well as in space and enemy-induced environments.

Space Sciences Laboratory: Magnetospheric, auroral and cosmic ray physics, wave-particle interactions, magnetospheric plasma waves; atmospheric and ionospheric physics, density and composition of the upper atmosphere, remote sensing using atmospheric radiation; solar physics, infrared astronomy, infrared signature analysis; effects of solar activity, magnetic storms and nuclear explosions on the earth's atmosphere, ionosphere and magnetosphere; effects of electromagnetic and particulate radiations on space systems; space instrumentation.